Acta Pharmaceutica Sinica B 2021;11(3):668–679

Chinese Pharmaceutical Association
Institute of Materia Medica, Chinese Academy of Medical Sciences

Acta Pharmaceutica Sinica B

www.elsevier.com/locate/apsb
www.sciencedirect.com

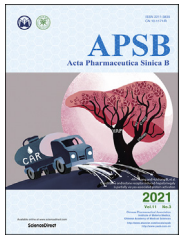

ORIGINAL ARTICLE

S-Allylmercaptocysteine improves alcoholic liver disease partly through a direct modulation of insulin receptor signaling

Pingping Luo[a,†], Ming Zheng[b,†], Rui Zhang[a], Hong Zhang[b], Yingxia Liu[c], Wei Li[d], Xiaoming Sun[e], Qian Yu[f], George L. Tipoe[f,*], Jia Xiao[a,f,*]

[a]*Clinical Medicine Research Institute, the First Affiliated Hospital of Jinan University, Guangzhou 510632, China*
[b]*Department of Interventional Surgery, the First Affiliated Hospital of Jinan University, Guangzhou 510632, China*
[c]*State Key Discipline of Infectious Diseases, Department of Infectious Diseases, Shenzhen Third People's Hospital, Shenzhen 518000, China*
[d]*Faculty of Pharmaceutical Sciences, Toho University, Chiba 2748510, Japan*
[e]*School of Integrative Pharmacy, Institute of Integrative Pharmaceutical Research, Guangdong Pharmaceutical University, Guangzhou 510000, China*
[f]*School of Biomedical Sciences, Li Ka Shing Faculty of Medicine, the University of Hong Kong, Hong Kong 999077, China*

Received 29 June 2020; received in revised form 31 August 2020; accepted 7 September 2020

Abbreviations: ADIPOQ, adiponectin; ALD, alcoholic liver disease; ALDH2, aldehyde dehydrogenase 2; ALT, alanine aminotransferase; AMPK, adenosine 5′-monophosphate (AMP)-activated protein kinase; AST, aspartate aminotransferase; ATGL, adipose triglyceride lipase; CPT1, carnitine palmitoyltransferase I; CYP2E1, cytochrome P450 2E1; FDA, U.S. Food and Drug Administration; FFA, free fatty acids; GRB14, growth factor receptor-bound protein 14; GSK3β, glycogen synthase kinase 3 beta; GTT, glucose tolerance test; HSL, hormone sensitive lipase; IGF-1, insulin-like growth factors-1; IL, interleukin; INSR, insulin receptor; IRS, insulin receptor substrate; IRTK, insulin receptor tyrosine kinase; LDLR, low-density lipoprotein receptor; LRP6, low-density lipoprotein receptor related protein 6; MTT, 3-(4,5-dimethyl-thiazol-2-yl)-2,5-diphenyl-tetrazolium bromide; NAC, *N*-acetyl-cysteine; NAFLD, non-alcoholic fatty liver disease; NAS, NAFLD activity score; NF-κB, nuclear factor kappa B; NIAAA, National Institute on Alcohol Abuse and Alcoholism; NRF2, nuclear factor erythroid 2-related factor 2; ORF, open reading frame; PA, palmitate acid; PPARα, peroxisome proliferator-activated receptor alpha; RER, respiratory exchange ratio; SAMC, *S*-allylmercaptocysteine; SPR, surface plasmon resonance; SREBP-1c, sterol regulatory element-binding protein 1c; TC, total cholesterol; TCF/LEF, T-cell factor/lymphoid enhancer factor; TG, triglyceride; TNF, tumor necrosis factor; TSA, thermal shift assay; WAT, white adipose tissues; WT, wild-type.

*Corresponding authors. Tel./fax: +86 20 85225180.
E-mail addresses: edwinsiu@connect.hku.hk (Jia Xiao), tgeorge@hku.hk (George L. Tipoe).
[†]These authors made equal contributions to this work.

Peer review under responsibility of Chinese Pharmaceutical Association and Institute of Materia Medica, Chinese Academy of Medical Sciences.

https://doi.org/10.1016/j.apsb.2020.11.006

KEY WORDS

Alcoholic liver disease;
S-Allylmercaptocysteine;
Insulin receptor;
Insulin resistance;
IRS-1;
AKT;
GSK3β;
Safety

Abstract Alcoholic liver disease (ALD) causes insulin resistance, lipid metabolism dysfunction, and inflammation. We investigated the protective effects and direct regulating target of *S*-allylmercaptocysteine (SAMC) from aged garlic on liver cell injury. A chronic ethanol-fed ALD *in vivo* model (the NIAAA model) was used to test the protective functions of SAMC. It was observed that SAMC (300 mg/kg, by gavage method) effectively ameliorated ALD-induced body weight reduction, steatosis, insulin resistance, and inflammation without affecting the health status of the control mice, as demonstrated by histological, biochemical, and molecular biology assays. By using biophysical assays and molecular docking, we demonstrated that SAMC directly targeted insulin receptor (INSR) protein on the cell membrane and then restored downstream IRS-1/AKT/GSK3β signaling. Liver-specific knock-down in mice and siRNA-mediated knock-down in AML-12 cells of *Insr* significantly impaired SAMC (250 μmol/L in cells)-mediated protection. Restoration of the IRS-1/AKT signaling partly recovered hepatic injury and further contributed to SAMC's beneficial effects. Continuous administration of AKT agonist and recombinant IGF-1 in combination with SAMC showed hepato-protection in the mice model. Long-term (90-day) administration of SAMC had no obvious adverse effect on healthy mice. We conclude that SAMC is an effective and safe hepato-protective complimentary agent against ALD partly through the direct binding of INSR and partial regulation of the IRS-1/AKT/GSK3β pathway.

1. Introduction

Alcoholic liver disease (ALD) is induced by acute or chronic excessive consumption of ethanol. Histopathological features range from alcoholic steatosis, alcoholic steatohepatitis to alcoholic cirrhosis, and even hepatocellular carcinoma[1]. Globally, excessive alcohol consumption accounts for approximately 3 million death in 2016[2]. The prevalence of ALD in the United States and European countries ranges from ∼5% to ∼6%[3]. Many risk factors, such as beverage type, consumption pattern, gender, age, race/ethnicity, genetics, obesity, and smoking, could significantly affect the pathogenesis of ALD[4]. Currently, there is no specific U.S. food and drug administration (FDA)-approved therapeutic intervention for the medical management of ALD patients, apart from abstinence of alcohol intake which is considered the most effective therapy. However, it often needs additional support from psychiatric interventions and lifestyle modifications. Successful drinking cessation not only reverses mild steatosis, but also improves survival in alcoholic cirrhotic patients[5]. Novel therapy with well-characterized molecular mechanisms and proven safety is urgently needed for ALD patients.

Ethanol consumption impairs insulin signaling and causes insulin resistance in the liver[6,7]. Insulin affects hepatocytes through the binding of cell surface insulin receptor (INSR), which activates insulin receptor substrate-1 (IRS-1) and substrate-2 (IRS-2) to functionally mediate glucose/lipid metabolism, hepatocyte proliferation, DNA synthesis, and cell cycle regulation[8]. Downstream signaling components of the INSR−IRS axis mainly consist of protein kinase B (AKT) and glycogen synthase kinase-3 beta (GSK3β). Appropriate activation of the AKT/GSK3β pathway is critical for precise energy metabolism and cell survival in the liver[9]. Restoration of insulin signaling, including AKT/GSK3β, has been proved to alleviate ALD-induced hepatic injury[10,11]. Thus, developing an effective and safe insulin signaling activator might be one of the novel treatment strategies for ALD.

S-allylmercaptocystein (SAMC) is a water-soluble component extracted from aged garlic. Several studies highlighted its anti-cancer properties against gastric[12], colon[13], prostate[14], ovarian[15], and thyroid cancer[16]. Our studies have shown the hepato-protective effects of SAMC on acute liver injury[17], non-alcoholic fatty liver disease (NAFLD)[18,19], and liver cancer[20]. We identified that cell membrane-bound receptor low-density lipoprotein receptor (LDLR)-related protein 6 (LRP6) was a direct target of SAMC probably through inhibiting the receptor-mediated downstream oncogenic pathways[19]. However, whether and how SAMC ameliorates ethanol-induced liver injury remain largely unknown. Our current study demonstrated that daily consumption of SAMC effectively protected the mice liver against chronic-binge ethanol consumption partially through restoration of insulin signaling in hepatocytes. SAMC directly bound to INSR and recovered downstream IRS-1/AKT/GSK3β phosphorylation. Exogenous activation of the IRS-1/AKT/GSK3β signaling further contributed to SAMC-mediated hepato-protection. Long-term administration of SAMC had no obvious adverse effect on healthy mice which suggests that SAMC is a safe hepato-protective complimentary agent for ALD therapy. To our best knowledge, SAMC is the first natural product with direct insulin receptor binding and insulin signaling restoration properties validated in animal models.

2. Materials and methods

2.1. Chemicals and reagents

SAMC powder (>95%) was provided by Wakunaga Pharmaceutical Co., Ltd. (Osaka, Japan). Pure ethanol was purchased from Guangzhou Chemical Reagent Factory (Guangzhou, China). All cell culture consumables and reagents were supplied by either Corning Incorporated (Corning, NY, USA) or Gibco (Carlsbad, CA, USA). Primary antibodies against adiponectin (ADIPOQ; #ab22554), phosphorylated AKT at Thr308 or Ser473 (pAKT; #ab38449 and #ab81283), total AKT (#ab8805), aldehyde dehydrogenase 2 (ALDH2; #ab154993), adipose triglyceride lipase (ATGL; #ab109251), phosphorylated adenosine

5′-monophosphate (AMP)-activated protein kinase at Ser487 (pAMPK; #ab131357), total AMPK (#ab32047), beta-actin (β-actin; #ab115777), cleaved caspase-3 (C-caspase-3; #ab2302), carnitine palmitoyltransferase I (CPT1; #ab128568), cytochrome P450 2E1 (CYP2E1; #ab28146), CD45 (#ab205718), phosphorylated glycogen synthase kinase 3 beta at Ser9 or Tyr216 (pGSK3β; #ab75814 and #ab75745), total GSK3β (#ab32391), nuclear factor erythroid 2-related factor 2 (NRF2; #ab156883), phosphorylated nuclear factor kappa B P65 subunit at Ser536 (pNF-κB P65; #ab86299), total NF-κB P65 (#ab16502), peroxisome proliferator-activated receptor alpha (PPARα; #ab24509), PPARγ (#ab59256), and sterol regulatory element-binding protein 1c (SREBP-1c; #ab28481) were purchased from Abcam (Cambridge, UK). Antibodies against phosphorylated hormone sensitive lipase at Ser563 (HSL; #4139), total HSL (#4107), phosphorylated IRS-1 at Ser302 (#2384), and total IRS-1 (#2382) were products of Cell Signaling (Shanghai, China). All antibodies are validated by their manufacturers (see corresponding product web pages) and in our pilot studies. The dilution ratios for all primary antibodies and secondary antibodies used in the current study were 1:1000 and 1:2000, respectively.

2.2. *Construction of AAV8-shInsr*

AAV was produced by transfection of AAV-293 cells with three plasmids namely an AAV vector expressing the shRNA to mouse *Insr*, AV helper plasmid (pAAV Helper) and AAV Rep/Cap expression plasmid. After transfection for 72 h, cells were collected and lysed using a freeze-thaw procedure. Viral particles were purified by an iodixanol step-gradient ultracentrifugation method. AAV was concentrated using a 100 kDa molecular-mass-cut off ultrafiltration device. The genomic titer was 2.5×10^{12}−5×10^{12} infectious units per mL as determined by quantitative PCR. To construct shRNAs, oligo-nucleotides that contained sense and antisense sequences were connected with a hairpin loop followed by a poly (T) termination signal. The sequence of the control shRNA was TTCTCCGAACGTGTCACGT. These shRNAs were ligated into an AAV8 vector expressing H1 promoter and EGFP.

2.3. *Animals and experimental design*

Male C57BL/6 wild-type mice (7-week old; 18−19 g) were purchased from Guangdong Medical Animal Centre (Guangzhou, China). Mice were acclimatized to their environment for 1 week before the experiments. Alcoholic liver injury was induced by using the National Institute on Alcohol Abuse and Alcoholism (NIAAA) model with minor modifications[21]. Briefly, mice (10/group) were initially fed *ad libitum* with the control Lieber-DeCarli diet for 5 days to allow acclimation to liquid diet. Then, the NIAAA groups (indicated as 'EtOH' group in figures) were fed with the Lieber-DeCarli diet containing 5% (*v*/*v*) ethanol for 10 days (first stage), while the control mice (indicated as 'Pair' group in figures) were pair-fed with the isocaloric control diet (same caloric content). Changes in body weight and food intake of each mouse were recorded every day. On Day 11, ethanol-fed and pair-fed mice were fed by gavage method in the early morning with a single dose of ethanol (the binge consumption; 5 g/kg body weight) or isocaloric maltose dextrin, respectively, and euthanized 9 h later. SAMC (300 mg/kg, in normal saline) regimens also fed by gavage method on Day 6 and administered every other day (indicated as 'EtOH + SAMC' group in figures). Pair-fed mice were fed by gavage method with the same volume of SAMC (indicated as 'Pair + SAMC' group in figures) or saline. Parallel experiments using *N*-acetyl-L-cysteine (NAC, 100 mg/kg, gavage, every other day; Sigma−Aldrich, St. Louis, MO, USA; #A9165)[22], resveratrol (0.0125%, *v*/*v*, of total diet, Sigma−Aldrich; #R5010)[23], and silibinin (Legalon®, SIL, 25 mg/kg, i.p. injection, every other day; Madaus, Cologne, Germany)[24] were also conducted using the same NIAAA model. For viral injections, mice were injected *via* the tail vein with 1×10^{12} genome copies of AAV8 control or AAV-shRNA (five per group). After 14 days, mice fasted for 4 h at the end of the dark cycle and then sacrificed to ensure the hepatic down-regulation of *Insr*. These mice were also subjected to NIAAA model and/or SAMC administration as described above. To verify the function of AKT activation, recombinant human insulin-like growth factor-1 (IGF-1, 100 μg/kg, i.p. injection; Sigma−Aldrich, #I8779) was administered every other day in conjunction with the start of ethanol consumption[22]. For long-term safety test, 300 mg/kg SAMC was administered every day for 90 days. After 90 days, tissues from the liver, heart, kidneys, and spleen were prepared for haematoxylin and eosin (H&E) histological evaluations and biochemical assays. The optimal dose of SAMC (300 mg/kg) was selected based on our previous liver disease studies[17−20]. All experimental procedures were approved by the Ethical Committee of Shenzhen Third People's Hospital, Shenzhen, China.

2.4. *Serum/hepatic biochemistry and cytokine measurements*

Serum levels of alanine aminotransferase (ALT), aspartate aminotransferase (AST), triglyceride (TG) and total cholesterol (TC) were measured using Hitachi LABOSPECT 008 (Hitachi High-Tech Co., Tokyo, Japan). Serum and hepatic cytokine levels were determined by using corresponding ELISA kits from Peprotech [Rocky Hill, NJ, USA; tumor necrosis factor (TNF)-α: #900-M54; IL-6: #900-M50]. Blood ethanol levels were measured 2 h after the binge gavage with the UV photometric method of Boehringer Diagnostica Mannheim GmBH and measured on an automated 717 clinical chemistry analyzer (Hitachi) at a wavelength of 365 nm. Hepatic TG contents were measured by a colorimetric TG assay kit from Sigma−Aldrich (#MAK266).

2.5. *Tissue histology*

Tissues were fixed in 10% phosphate-buffered formalin and embedded in paraffin blocks. A thickness of 5 μm of tissue section was cut and stained with H&E and oil red O (Sigma−Aldrich) for histological analysis using a LEICA Qwin Image Analyzer (Leica Microsystems Ltd., Milton Keynes, UK). The NAFLD activity score (NAS) of each group was calculated as previously described[25]. For adipose tissue assays, tissues were also fixed in 10% formalin and then cut at 7 μm for H&E staining and quantification. Five tissue sections from each group were selected, and the diameters of 40 adipocytes from each tissue section were measured. For lipolysis assay, epididymal white adipose tissues (WAT) were cut from mice and washed in pre-warmed Dulbecco's PBS containing 100 U/mL penicillin and 100 mg/mL streptomycin. Connective tissue and blood vessel were removed. After that, 20 mg of adipose tissue explants were placed into 24-well

plates, cut into small pieces, and cultured in 200 μL of Dulbecco's modified Eagle's medium (DMEM). Released free fatty acids were measured by using a commercial kit from BioVision (Milpitas, CA; #K612-100). Immunohistochemistry of CD45 in mice liver sections was conducted by using CD45 antibody (Abcam, 1:5000 dilution; #ab208022) with DAB (Abcam) color development.

2.6. Respiratory exchange ratio and energy expenditure

Respiratory exchange ratio (RER) and energy expenditure were measured by using a Comprehensive Laboratory Animal Monitoring System (Columbus Instruments, Columbus, OH, USA). Four mice per group were housed individually and assessed by indirect calorimetry over 48 h (last 2 days of the NIAAA model) and maintained at 24 °C under at 12-h:12-h light−dark cycle. An RER of 0.7 indicates that fat is the predominant fuel source, while an RER closer to 1.0 indicates that carbohydrate is the primary fuel[26].

2.7. Insulin resistance measurements

A glucose tolerance test (GTT; 2.5 g/kg glucose, i.p. injection) was performed on the 6-h fasted mice (from AM 8:00 to PM 2:00) by using a glucometer from Roche (Accu-Chek Perfoma, Basel, Switzerland) at blood collecting time points of 0, 30, 60, 90, 120 min ($n = 5$; extra mice in parallel experiments). For insulin challenge experiments, the mice were i.p. injected with 2 U/kg recombinant insulin (Sigma−Aldrich; #91077C) 20 min before tissue collection. Plasma insulin level was measured using an ELISA kit from BioVision (#K4271) ($n = 5$; extra mice in parallel experiments).

2.8. Surface plasmon resonance (SPR) and thermal shift assay (TSA)

The possible direct interaction between SAMC and insulin receptor was validated by using both SPR and TSA assays. SPR was conducted at 25 °C on a BIAcore T100 SPR instrument (GE Healthcare, Chicago, IL, USA). SPR running buffer contained 50 mmol/L HEPES (pH 7.5), 150 mmol/L NaCl, 3 mmol/L EDTA and 0.005% (*v*/*v*) Tween-20 and was prepared immediately before measurement. BIAcore sensor chip CM5 was activated for 5−10 min in a 1:1 mixture of 0.1 mol/L *N*-hydroxysuccinimide and 0.1 mol/L *N*-ethyl-*N*′-(3-diethylaminopropyl)-carbodiimide at a flow rate of 10 μL/min. Recombinant mouse insulin receptor protein (Chinese hamster ovary cell-derived eukaryotic protein, R&D systems, Minneapolis, MN, USA) was immobilized *via* amine coupling on a flow cell of the chip. The remaining binding sites on the chips were blocked by 1 mol/L ethanolamine (pH 8.5) at a flow rate of 10 μL/min for 5 min. Control sensorgrams, obtained on an empty flow cell where the coupling reaction had been conducted in the presence of coupling buffer alone, were always subtracted from binding responses. SAMC was diluted in the running buffer and then injected at different concentrations (100, 200 and 400 μg/mL) and passed over adjacent target and control flow cells at a flow rate of 20 μL/min for 180 s. After a 5-min dissociation, the bound analytes were removed by a 20-s wash with 20 mmol/L NaOH.

For TSA, we used 0.04 mg/mL insulin receptor protein with or without 0.2 mmol/L of SAMC in PBS. Data were analyzed with the differential scanning fluorimetry analysis tool (Microsoft Excel based) using the curve-fitting software XLfit 5 (www.idbs.com, ID Business Solutions Ltd.).

2.9. Protein structure modelling

To predict the binding properties of SAMC on INSR, we used the crystal structure of INSR:GRB14 complex from Protein Data Bank (PDB) database (PDB code: 2AUH and 2Z8C) since previous studies demonstrated that growth factor receptor-bound protein 14 (GRB14) was a tissue-specific negative regulator of INSR signaling, and the inhibition was mediated by the BPS (between PH and SH2) region[27]. Targeting the insulin receptor tyrosine kinase domain (IRTK)−GRB14 interaction, in order to relieve the GRB14 inhibitory action on the IRTK, has been considered to be a potential therapeutic strategy to improve insulin signaling[28]. The binding pose of compound in the binding site of IRTK was predicted by the Autodock (version 4.2.6; The Scripps Research Institute, La Jolla, CA, USA). Then, the protein and compound were prepared by AutoDockTools software (version 1.5.6; The Scripps Research Institute).

2.10. Cell culture and transfection

The mouse normal hepatocyte line AML-12 was purchased from the Cell Bank of Type Culture Collection of Chinese Academy of Sciences (Shanghai, China). Cells were cultured in DMEM with 10% (*v*/*v*) fetal bovine serum (FBS) at 37 °C with 5% CO_2 using a cell incubator. Cells were treated after they reached a confluence of 60%−70%. To induce *in vitro* ALD-like injury of AML-12 cells, we co-treated cells with 250 mmol/L ethanol and 0.25 mmol/L palmitate acid (PA; Sigma−Aldrich; #P0500) for 24 h[29]. To investigate the effects of SAMC on AML-12 cells, different doses of SAMC were added along with concurrent PA and ethanol for a 24-h incubation. Of note, since there is no FDA-approved ALD drug and the efficacy of steroids, anti-TNF agents, growth factors, or antioxidants in treating ALD is controversial and heavily depends on disease stage and host conditions[30], we did not set a positive drug to make a comparison with SAMC in the pharmacodynamic experiment. Knockdown of *Insr* was achieved by transfection of Rosetta Predictions siRNA (Sigma−Aldrich; #NM_010568) with Lipofectamine 3000 reagent (Thermo-Fisher, Waltham, MA; #L3000001). Overexpression of *Irs-1* and *Akt* in AML-12 cells was conducted by using pCDNA3.1 plasmid harboring full-length sequences of open reading frame (ORF) of mouse *Irs-1* (NCBI Reference Sequence: NM_010570.4) and *Akt 1* (NCBI Reference Sequence: NM_009652.3) with Lipofectamine 3000.

2.11. Cell viability/apoptosis

The 3-(4,5-dimethyl-thiazol-2-yl)-2,5-diphenyl-tetrazolium bromide (MTT) cell viability assay was conducted as described in previous report[17]. After drug treatment, Hoechst 33342 (5 μg/mL) and propidium iodide (5 μg/mL) were added to each well to stain live cells. Quantifications of apoptotic ratio and caspase-3/7/8 activity were conducted as previously described[20].

2.12. Caspase-3/7 activity and P65 activity assay

Activities of caspase-3/7 from cell lysates after treatment were measured using Cell Meter Caspase-3/7 Activity Apoptosis Assay Kit (AAT Bio., Sunnyvale, CA, USA; #22795) according to the

user manual. Final results were read at 520 nm in a micro-plate reader (Bio-Rad) and expressed as fold change in caspase-3/7 activity relative to the control. To test the cellular NF-κB P65 activity, a NF-κB P65 Transcription Factor Assay Kit (Abcam; #ab133112) was used according to user's instructions.

2.13. Quantitative real-time PCR

Total RNA was extracted from fresh liver tissue samples or cell lysates by using the CellAmp™ Direct RNA Prep Kit (Takara Bio, Inc., Shiga, Japan; #3732). The first strand cDNA was synthesized from total RNA using a PrimeScript™ RT Reagent Kit (Takara; #RR037) following the manufacturer's instructions. qPCR reaction was performed with the SYBR Premix Taq Quantitative PCR Kit (Takara Bio, Inc.), according to the manufacturer's instructions, on a MyiQ2 real-time quantitative PCR machine (Bio-Rad, Berkeley, CA, USA). Primer information is as listed in Supporting Information Table S1. Glyceraldehyde-3-phosphate dehydrogenase (*Gapdh*) was amplified as an internal control. The relative quantification of mRNA expression levels was done according to the $2^{-\Delta\Delta Ct}$ method. All real-time PCR procedures, including the design of primers, validation of PCR environment and quantification methods, were performed according the MIQE guideline[31].

2.14. Protein extraction and Western blot

After treatments, cells or liver tissues were washed with sterile phosphate buffer saline (PBS) for three times and then subjected to total protein extraction by using a RIPA kit from Sigma−Aldrich. For secreted protein, culture medium was collected and centrifuged for RIPA extraction. Then protein samples were quantified with BCA reagent from Bio-Rad. Western blot analyses of all proteins were performed as described using β-actin as the internal control.

2.15. In vitro glucose uptake assay

Cell-based glucose uptake assay was conducted by using a commercial kit from Cayman Chemical (Ann Arbor, MI, USA; #10009582) according to manufacturer's instructions. Briefly, AML12 cells were seeded at 2.5×10^4 cells/well in a 96-well plate and incubated overnight. On the next day, cells were treated with ethanol + PA and/or SAMC (250 μmol/L) for 24 h in glucose-free culture medium. Ten minutes before the end of the treatment (half cells were stimulated with 20 nmol/L for 10 min), cells were incubated with 200 μg/mL 2-(*N*-(7-nitrobenz-2-oxa-1,3-diazol-4-yl)amino)-2-deoxyglucose (2-NBDG) for 8 h. Culture plates were then centrifuged for 5 min at 400×*g* at room temperature, and the supernatants were aspirated. Cells were incubated with reaction buffer for 10 min and then the glucose uptake was measured with fluorescent filters (excitation/emission = 485 nm/535 nm).

2.16. TCF/LEF reporter luciferase assay

The activity of β-catenin activity was measured by a luciferase reporter assay of T-cell factor/lymphoid enhancer factor (TCF/LEF)-dependent transcription with Cignal TCF/LEF Reporter Kit (Qiagen, Valencia, CA, USA). *Renilla* luciferase construct was also co-transfected into each well for normalization. The luciferase activity was measured using the dual-luciferase reporter assay system (Promega, Fitchburg, WI, USA).

2.17. Statistical analysis

Data were expressed as mean ± standard error of mean (SEM). All data in this study were normally distributed as confirmed by the Shapro-Wilk test and P−P plot using SPSS software package. Statistical differences for two group comparison were determined using independent-samples *t*-test (SPSS version 24.0 for Windows, International Business Machines Corporation, Armonk, NY, USA). Differences are considered significant if the *P* value is <0.05.

3. Results

3.1. SAMC ameliorated hepatic injury after chronic ethanol consumption

During an 11-day of ethanol consumption, mice showed significant reduction in body weight. Daily gavage of 300 mg/kg SAMC effectively restored part of the lost body weight without affecting the weight gain in healthy mice (Fig. 1A). Of note, ethanol consumption reduced respiratory exchange ratio (RER), and energy expenditure of mice (the diet intake was manually maintained equally among groups, according to the NIAAA model guidelines). Supplementation with SAMC did not alter those parameters, implying that the body weight restorative effects might be attributed to other mechanisms, such as lipid metabolism correction and adipose tissue regulation (Supporting Information Fig. S1). As expected, the chronic-binge ethanol consumption significantly increased the liver weight, liver-to-body ratio, free fatty acids (FFAs) levels of mice, serum levels of ALT and AST which indicated a more severe status of hepatic injury, and the markedly elevated levels of TC and TG suggesting a state of dysregulated lipid metabolism. This was further validated by liver histology and TG level results (Fig. 1B−D, and G). We also demonstrate that during ALD progression, serum levels of key cytokines (TNF-α and IL-6) were also markedly elevated, indicating the occurrence of inflammation (Fig. 1E). Co-treatment with SAMC effectively ameliorated those abnormalities without changing the basal conditions. Blood ethanol level in ALD mice was reduced by SAMC (388.6 ± 18.5 *vs*. 325.2 ± 15.7 mg/dL; $P < 0.05$). In addition, protein level alterations of assessed genes involved in lipid metabolism (SREBP-1C, CPT1, and ADIPOQ), ethanol/drug metabolism (ALDH2 and CYP2E1), antioxidant markers (CAT and NRF2), apoptosis (cleaved caspase-3), metabolism-related pathways (AMPK and NF-κB P65 subunit) were also reversed by SAMC co-administration during the establishment of the NIAAA model (Fig. 1F). Importantly, we compared the hepato-protective effects of SAMC with other commonly used agents (NAC, resveratrol, and silibinin) on the ALD-induced liver injury model and found that SAMC had the best ameliorative effect, in terms of parameters of hepatic histology, TG, and inflammation amongst those protective agents (Supporting Information Fig. S2).

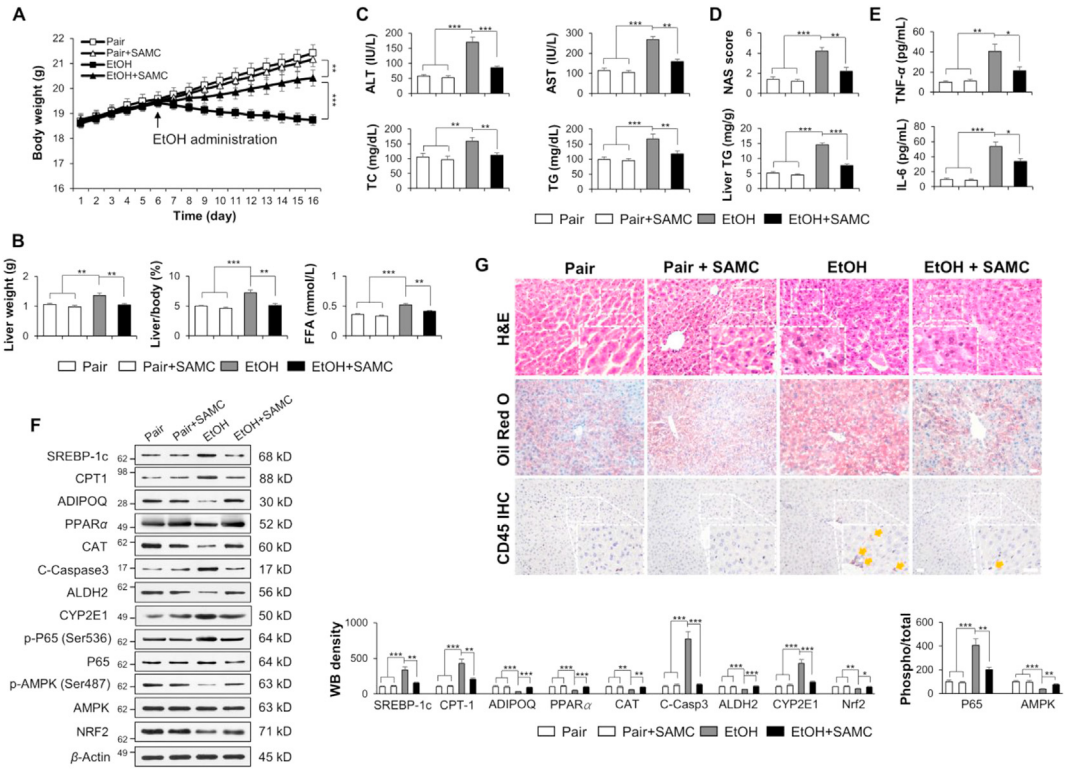

Figure 1 SAMC supplementation improved ALD-induced liver injury. (A) SAMC partially recovered reduced body weight of mice by ethanol administration from Day 6 to Day 16. (B) Changes of liver weight, liver-to-body weight ratio, and free fatty acid (FFA) of mice. (C) Changes of serum chemistry (ALT, AST, total cholesterol, and triglyceride) of mice. (D) NAS scorings and liver triglyceride (liver TG) results from each group of mice. (E) Changes of serum inflammatory mediators (TNF-α, and IL-6) of mice. (F) Representative Western blot results ($n = 3$) and densitometry analysis of mice hepatic markers (G) Representative H&E, oil red O, and CD45 immunohistochemical staining images of the mice liver (yellow arrows indicate typical CD45 signals). Data are expressed as mean ± SEM ($n = 5$). Significant differences between the indicated groups: $^{*}P < 0.05$, $^{**}P < 0.01$, $^{***}P < 0.001$. Scale bar = 20 μm.

3.2. *Insulin receptor signaling and adipose tissue lipolysis mediated SAMC-induced hepato-protection*

Like NAFLD, chronic ethanol consumption is also able to cause insulin resistance[11]. Thus, we examined the possible beneficial effects of SAMC co-treatment on insulin resistance. Results show that ethanol feeding induced evident insulin resistance, as suggested by impaired glucose metabolism and elevated serum insulin level. SAMC partially ameliorated the insulin resistance caused by ALD. Interestingly, vehicle−SAMC administration also improved the basal insulin sensitivity of the healthy mice (Fig. 2A and B). In addition, impaired AKT (both the phosphorylated forms at Thr308 and Ser473) and GSK3β (both the phosphorylated forms at Ser9 and Tyr216) signaling was also recovered by SAMC co-treatment, when it was stimulated by insulin. Interestingly, ethanol alone reduced the phosphorylation of GSK3β, but not AKT (Fig. 2C). It should be noted that neither ethanol consumption nor SAMC treatment influenced the mRNA and protein expression levels of both *Insr* and insulin receptor substrate-1 (*Irs-1*) in the mice liver. Induction of ALD inhibited the phosphorylation of IRS-1, which was fully restored by the co-treatment with SAMC (Supporting Information Fig. S3). To further investigate the role of insulin receptor (INSR), an AAV8-ligated *Insr* shRNA was injected to specifically knockdown the hepatic expression of *Insr* at both transcriptional and translational levels in mice, without influencing its levels in the brain, heart, white adipose tissue (WAT), and muscle (Fig. 2D). Of note, liver-specific knockdown of *Insr* (LIRKD) not only aggravated the ALD-induced elevation of serum chemistry, liver histology, systemic inflammation, and insulin resistance, but also significantly impaired the ameliorative effects of SAMC on those parameters (Fig. 2B−H). Importantly, there were statistically significant differences in those parameters between the ethanol and ethanol + SAMC groups in *Insr* deficiency mice, implying that although INSR was involved in SAMC-mediated protection, other mechanisms may also account for the amelioration of ethanol-induced injury as well.

It has been reported that chronic ethanol exposure induced adipose lipolysis and promoted hepatosteatosis[32]. To test the contribution of adipose tissue and SAMC's possible curative effects, we measured the changes of mass and adipocyte size of all of the three major abdominal fat depots, including epididymal, perirenal, and mesenteric white adipose tissue (WAT). Alcohol exposure significantly reduced both the mass and adipocyte size of those tissues and, as expected, co-treatment with SAMC restored the reductions (Fig. 3A and B). We also found that fatty acid released from freshly isolated epididymal WAT was markedly increased after chronic ethanol administration and alleviated by SAMC co-treatment (Fig. 3C). In addition, mice fed with ethanol exhibited upregulated adipose triglyceride lipase (ATGL) expression, increased phosphorylation level of hormone sensitive lipase (HSL), and suppressed peroxisome proliferators-activated receptors gamma (PPARγ) expression, indicating an enhanced lipolysis status. SAMC treatment significantly ameliorated such transitions (Fig. 3D). In summary, we show that insulin receptor

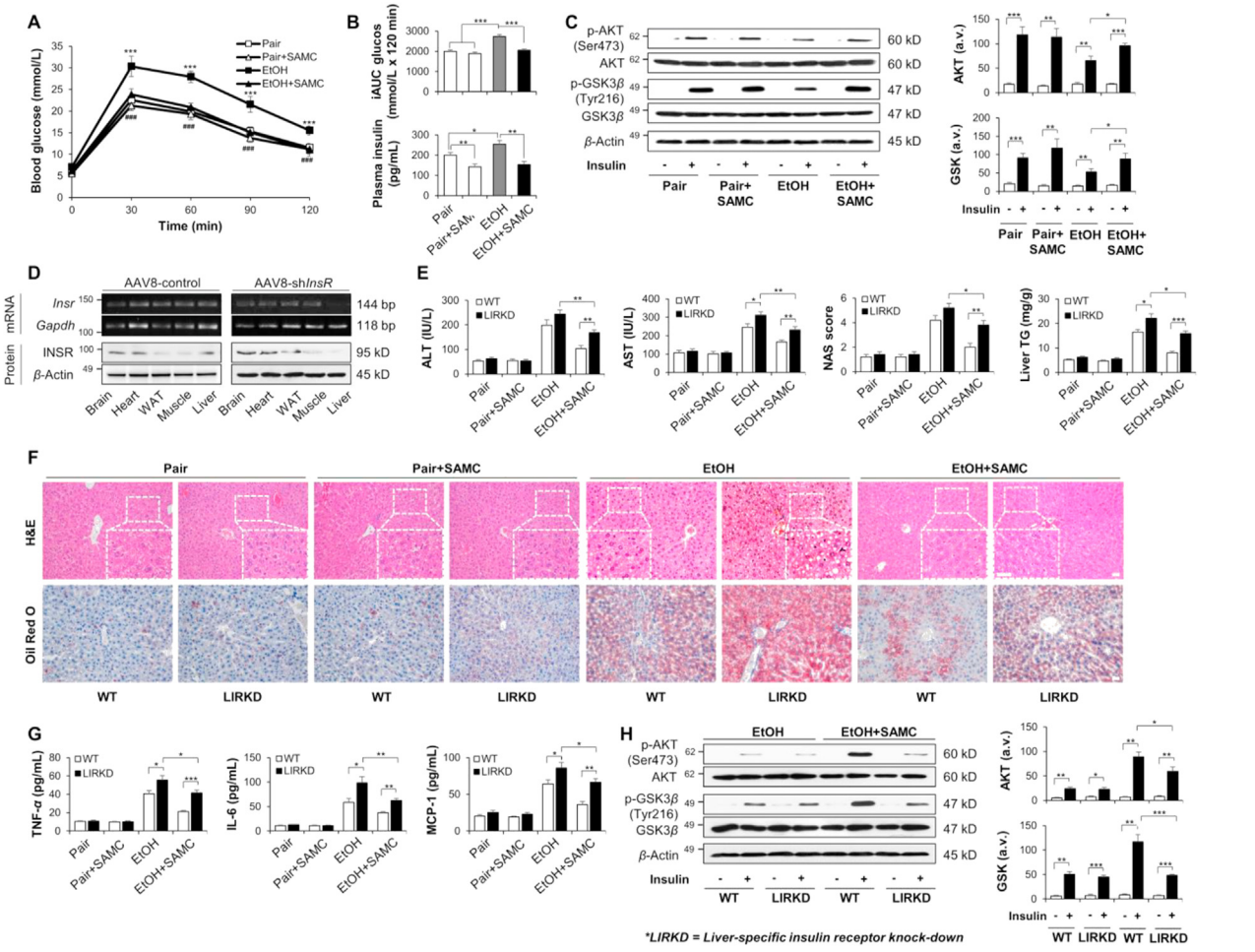

Figure 2 SAMC-mediated hepato-protective effect was insulin receptor (INSR)-dependent. (A) Results of glucose tolerance test (GTT). (B) Incremental area under the curve (iAUC) for blood glucose level and plasma insulin level between 30 and 60 min of GTT. (C) Representative images and corresponding quantitative data of phosphorylated and total AKT/GSK3β in all groups of mice ($n = 3$). For pAKT, only Ser473 data are presented since Thr308 had similar results and, for GSK3β, only Tyr216 data are shown since Ser 9 exhibited similar results. (D) Liver-specific knockdown efficacy at both transcriptional and translational levels of INSR (insulin receptor) after AAV8-sh*InsR* transfection in mice ($n = 3$). (E) Changes of serum chemistry (ALT and AST) NAS scorings and liver triglyceride (liver TG). (F) Representative H&E and oil red O staining images of liver sections. (G) Changes of serum inflammatory mediators (TNF-α, IL-6, and MCP-1) (H) Representative images and corresponding quantitative data of phosphorylated and total AKT/GSK3β in all groups of mice with or without INSR liver-specific knockdown ($n = 3$). For pAKT, only Ser473 data are presented since Thr308 had similar results and, for GSK3β, only Tyr216 data are shown since Ser9 exhibited similar results. Data are expressed as mean ± SEM ($n = 5$). Significant differences between the indicated groups: $^*P < 0.05$, $^{**}P < 0.01$, $^{***}P < 0.001$. Scale bar = 20 μm. LIRKD, liver-specific insulin receptor knockdown.

signaling and adipose lipolysis participated in SAMC-mediated protection against ALD. It should be noted that, since mice were still considered juvenile (7-week old) with the possible capacity to grow and malnourishment was a feature of the NIAAA feeding, thus the lack of body weight gain and increase of adipose mass could be possibly attributed to both ethanol intoxication and malnourishment.

3.3. *SAMC directly targeted insulin receptor protein*

To further investigate the direct interaction between SAMC and insulin receptor protein, we performed biophysical assays, TSA and SPR, by using recombinant INSR protein from a eukaryotic expression system. Results from TSA found that upon binding with SAMC, the melting temperature of INSR was elevated from ~56 to ~60 °C (Fig. 4A). Moreover, the SPR assay demonstrates that SAMC directly interacted with INSR in a positive dose-dependent manner (Fig. 4B). The docking prediction results reveal that SAMC compound formed three key hydrogen bonds with the residues of Arg1164, Lys1182 and Asp1183 of INSR. In addition, allylthio formed hydrophobic interaction with Le1171, Met1176, and Phe1186 residues. Previous study reported that inhibitor (S91) of the INSR targeted the catalytic binding site of the IRTK domain[33]. Thus, we hypothesized that SAMC bound to a novel binding site of GRB14-IRTK interface to disrupt the interaction between GRB-14 and IRTK (Fig. 4C and Supporting Information Fig. S4).

3.4. *INSR functionally mediated SAMC-induced hepatocyte protection via modulation of insulin resistance and lipid metabolism*

To further examine the role of INSR in SAMC-induced hepatocyte protection, we employed a PA and ethanol concurrent ALD-like

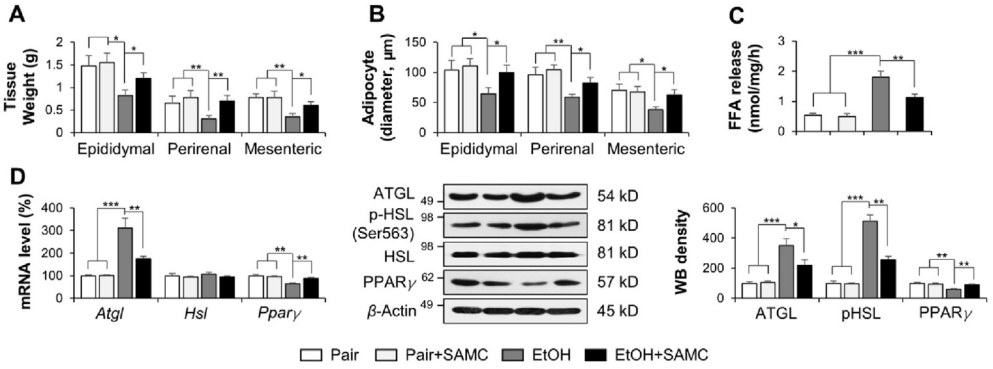

Figure 3 Effects of ethanol consumption and SAMC co-treatment on mice white adipose tissue (WAT) lipolysis. Changes of (A) abdominal WAT tissue weight and (B) adipocyte size (diameter) in mice treated with a chronic-binge alcoholic liver injury model (the NIAAA model) in the absence or presence of SAMC co-treatment ($n = 4$). (C) Fatty acid released from epididymal WAT cut from mice and them cultured in DMEM for 2 h. (D) Key markers expression from epididymal adipose tissue extracted from mice at both transcriptional ($n = 4$) and translational levels ($n = 3$). The immunoblot bands were quantified by densitometry analysis. Data are expressed as mean ± SEM. Significant differences between the indicated groups: $^{*}P < 0.05$, $^{**}P < 0.01$, $^{***}P < 0.001$.

AML-12 cell model. By measuring cell viability, apoptotic ratio, accumulation of lipid droplet, and caspase-3/7 activity, we observed that a 24-h co-incubation with 250 μmol/L SAMC exhibited significant improvement on chemical-induced cell damages (EC_{50} = 178.4 μmol/L for cell viability recovery, Supporting Information Fig. S5A). We also individually investigated the contribution of ethanol or PA to AML-12 damage and found that both agents could induce cell death, but could not replicate the phenotypic features of ALD mice at the same time (*i.e.*, induction of ethanol toxicity and lipotoxicity concurrently; Fig. S5B). In line with the *in vivo* results, neither cell injury induction by PA/ethanol nor co-treatment with SAMC altered the mRNA and protein expressions of *Insr* and *Irs-1* in AML-12 cells. Only the concurrent treatment with PA and ethanol reduced the phosphorylation level of IRS-1, which was then recovered by the addition of SAMC in the culture medium (Supporting Information Fig. S6). Then we transfected the siRNA of *Insr*, which effectively knocked-down the endogenous expression of *Insr* in AML-12 cells without affecting cell viability and apoptosis (Fig. 5A and B), prior to cell damage induction and SAMC co-treatment. Of note, knockdown of *Insr* significantly aggravated PA/ethanol-induced cell death and lipid accumulation. It also abolished the cell protective effects of SAMC (Fig. 5C and D). Indeed, deficiency of *Insr* impaired the insulin signaling (*i.e.*, phosphorylation of AKT and GSK3β upon insulin stimulation) in cells, which also counter-acted the recovery effects from SAMC on insulin signaling (Fig. 5E). To further prove this finding, we characterized the insulin-mediated glucose uptake, expressional changes of insulin-sensitive ADIPOQ, and lipid metabolism-related markers SREBP-1C, ACC, and CPT1 after PA/ethanol and SAMC treatments. Induction of ALD-like damage in cells significantly reduced insulin-stimulated glucose uptake, decreased ADIPOQ and CPT1 expressions, while elevated the expressions of lipid synthesis markers SREBP-1C and ACC. Although co-treatment with SAMC significantly alleviated these dysregulations, knockdown of *Insr* impaired the cellular protection of SAMC (Fig. 5F and G). Since we reported that SAMC could regulate NF-κB and WNT pathways[20], we also measured the activity changes of P65 and TCF/LEF in cells. It was exhibited that ethanol/PA promoted P65 activity but inhibited β-catenin activity, which were effectively reversed by SAMC. Deficiency of *Insr* potentiated the dysregulation caused by ethanol/PA, and impaired SAMC's protection (Supporting Information Fig. S7). This finding is consistent with previous reports showing suppressed β-catenin translocation in an ALD rat model[34] and IRS1/2 promotes WNT/β-catenin signaling by stabilizing DVL2[35].

To further examine the roles of insulin signaling in SAMC-mediated protection, we overexpressed *Irs-1* and/or *Akt* before cell damage and SAMC induction in AML-12 cells. Overexpressing either or both genes did not influence AML-12 cell viability and apoptotic ratio (data not shown). It was interesting that overexpression of *Akt* partially restored cell functions after PA/ethanol administration (Fig. 6). Co-overexpression of *Irs-1* and *Akt* showed better ameliorative effects than *Irs-1* or *Akt* overexpression alone. Co-treatment with SAMC further enhanced these protective effects (Fig. 6). We also tested the function of AKT activation by IGF-1 injection in the NIAAA mice model, with or without SAMC co-treatment. As expected, activation of AKT exhibited similar alleviative effects on ethanol-induced liver injury as SAMC. Concurrent IGF-1 and SAMC exhibited the most protective outcomes (Supporting Information Fig. S8). Overall, our data indicate that insulin signaling partially contributed to SAMC-induced hepato-protective effects against ALD.

3.5. *Long-term application of SAMC was safe in healthy animals*

We also checked the long-term (90-day continuous usage; 300 mg/kg, in normal saline; every other day gavage) safety of SAMC administration in healthy mice. We found no evidence of cell injury (H&E staining) in the mice liver, kidneys, spleen, and heart (Supporting Information Fig. S9A). In addition, when compared with the control group, levels of serum ALT, AST, FFA, and blood urea nitrogen (BUN) had no significant increase, implying a healthy status of these mice after long-term utilization of SAMC (Fig. S9B).

4. Discussion

Insulin resistance is a complex metabolic disorder induced by many factors such as ectopic lipid metabolites, endoplasmic

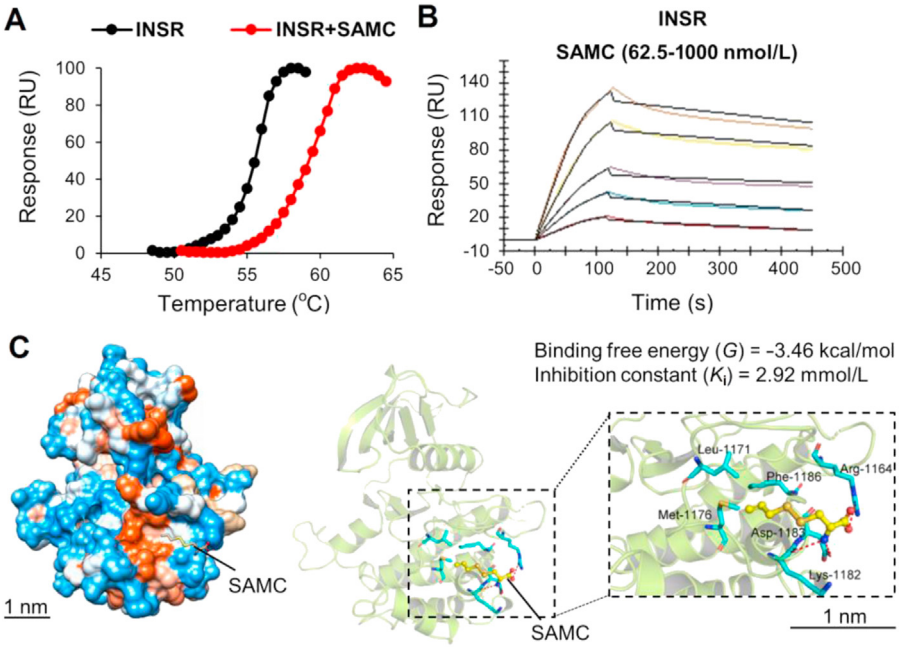

Figure 4 Insulin receptor was the direct binding cell membrane protein of SAMC. (A) and (B) TSA results of insulin receptor in the presence or absence of SAMC, and SPR results of the direct interaction between insulin receptor and 62.5−1000 nmol/L SAMC. (C) The proposed complex of SAMC with the ligand-binding pocket of insulin receptor. The ribbon structure displays the predicted bonds between SAMC and insulin receptor.

reticulum, and innate immune activation. In the liver, ectopic lipid accumulation is one of the most important causes of insulin resistance, which mainly results in reduced glycogen synthesis/storage and a failure to suppress the production and release of glucose from the liver into the blood circulation[36]. Inhibited INSR pathway leads to increased lipogenesis and decreased lipolysis in the liver which directly causes steatosis and subsequent inflammation[37−39]. Both acute and chronic ethanol consumptions are reported to induce insulin resistance and detailed molecular mechanisms remain inadequate[40]. Interestingly, insulin resistance triggered by NAFLD could in turn increase the blood ethanol level by an insulin-dependent impairment of alcohol dehydrogenase activity in liver tissue rather than from an increased endogenous ethanol synthesis[41]. Application of insulin sensitizer (*e.g.*, PPAR agonist) is shown to ameliorate hepatic insulin resistance, alcoholic steatohepatitis, and non-alcoholic steatohepatitis[42,43]. As a proven antioxidant and anti-inflammatory natural product, SAMC has been demonstrated to modulate the dysregulated lipid metabolism and prevent cell death in the chemical-induced liver injury and NAFLD models[17−19]. Although we found that LRP6 is a direct binding receptor of SAMC in hepatoma cells[20], the exact regulatory mechanisms of SAMC in metabolic liver diseases are still largely unknown. By using biophysical assays, protein binding prediction and liver specific knockdown, we revealed that INSR was a direct binding receptor of SAMC on the hepatocyte membrane and SAMC could restore suppressed insulin signaling during ALD development. More importantly, concurrent supplementation with SAMC and AKT agonist IGF-1 synergistically improved the liver injury in our NIAAA model which indicated the possible involvement of the insulin signaling in ALD progression and SAMC-mediated protective effects (Fig. S8).

Currently, there is no FDA-approved specific drug agent for ALD, but several targeted treatments are under development including corticosteroids, anti-TNF antibodies, pentoxifylline, and absorbable antibiotics[1,44]. Since oxidative stress is a key mechanism that drives the development of early ALD, particularly steatosis, the possibility of consuming antioxidants, either synthesized or from natural products attracts research attention. Although NAC has been suggested as the best candidate, NAC-based antioxidant therapies could not improve severe forms of alcoholic hepatitis in randomized studies[45,46]. Other natural products, such as resveratrol[47], silymarin[48], and green tea-derived EGCG[49], were characterized as effective hepato-protective agents against ALD. However, their targeted 'immediate molecules' on the cell membrane and therapeutic efficacy in ALD patients were not well studied. In the present study, SAMC was shown to possess comparable ameliorative effect, if not significantly better than those agents on cell death, oxidative stress, inflammation, and lipid dysregulation caused by chronic ethanol consumption. There might be other regulating mechanisms besides INSR binding, and our present study at least in part demonstrated the direct regulatory signaling pathway of SAMC in chronic ALD.

Admittedly, it could be shown from the results that compared the ethanol-treated *Insr* knockdown mice, SAMC still exhibited hepato-protective effects (*e.g.*, histology and inflammation) which implies the possible involvement of IR-independent pathways (*e.g.*, CYP2E1 pathway)[50]. As a natural hepato-protective ingredient, SAMC is highly possible to regulate a number of pathways involved in hepatic ethanol intoxication, lipid metabolism, and cellular inflammation through direct interactions with targets other than insulin receptor (*e.g.*, LRP receptors as we reported)[20]. Thus, there may be other mechanisms underlying the protection of SAMC against ALD, such as modulation of WNT signaling, as well as NF-κB and autophagy machine, as we previously reported[19]. An unbiased membrane proteomic assay is necessary to identify novel targets of SAMC in liver cells. Furthermore,

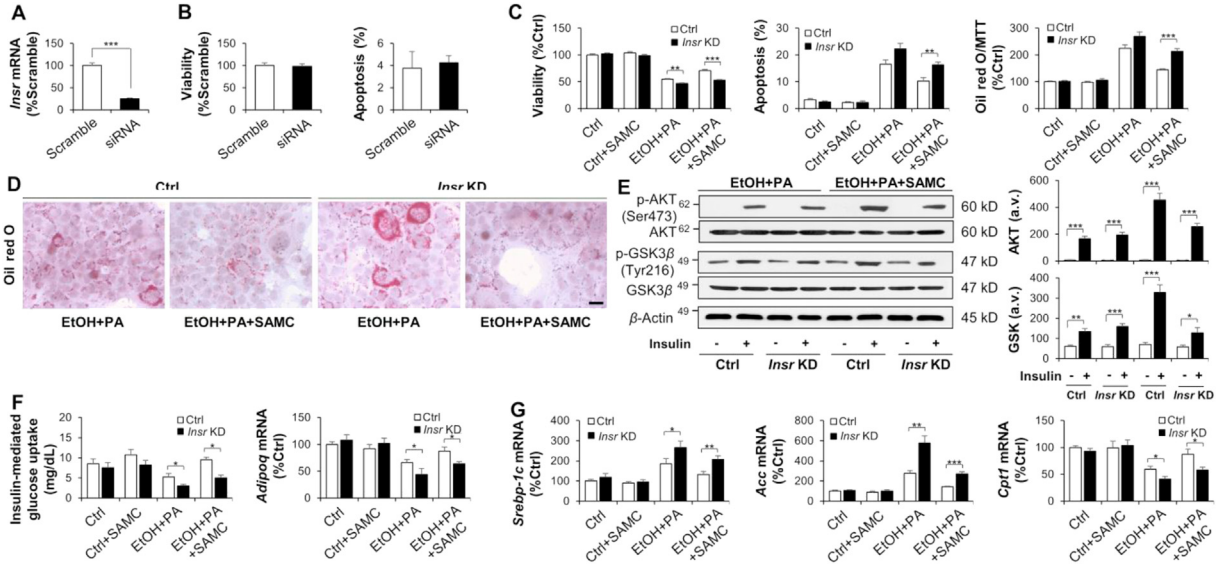

Figure 5 Insulin receptor and downstream signaling mediated hepatocyte protective effect of SAMC. (A) Test of knockdown efficacy of insulin receptor (*Insr*) in mice normal hepatocyte line AML-12. (B) Effects of *Insr* knockdown on AML-12 viability and apoptotic ratio. (C) Changes of cell viability and apoptotic ratio. (D) Representative oil red O staining images. (E) Representative images and corresponding quantitative data of phosphorylated and total AKT/GSK3β ($n = 3$). (F) Glucose uptake ability and *Adipoq* mRNA. (G) *Srebp-1c*, *Acc*, and *Cpt1* mRNAs when AML-12 cells were treated with cell injury induction combinations (palmitate acid + ethanol) and/or SAMC, in the absence or presence of *Insr* knockdown. Data are expressed as mean ± SEM ($n = 4$). Significant differences between the indicated groups: $^{*}P < 0.05$, $^{**}P < 0.01$, $^{***}P < 0.001$. Scale bar = 50 μm.

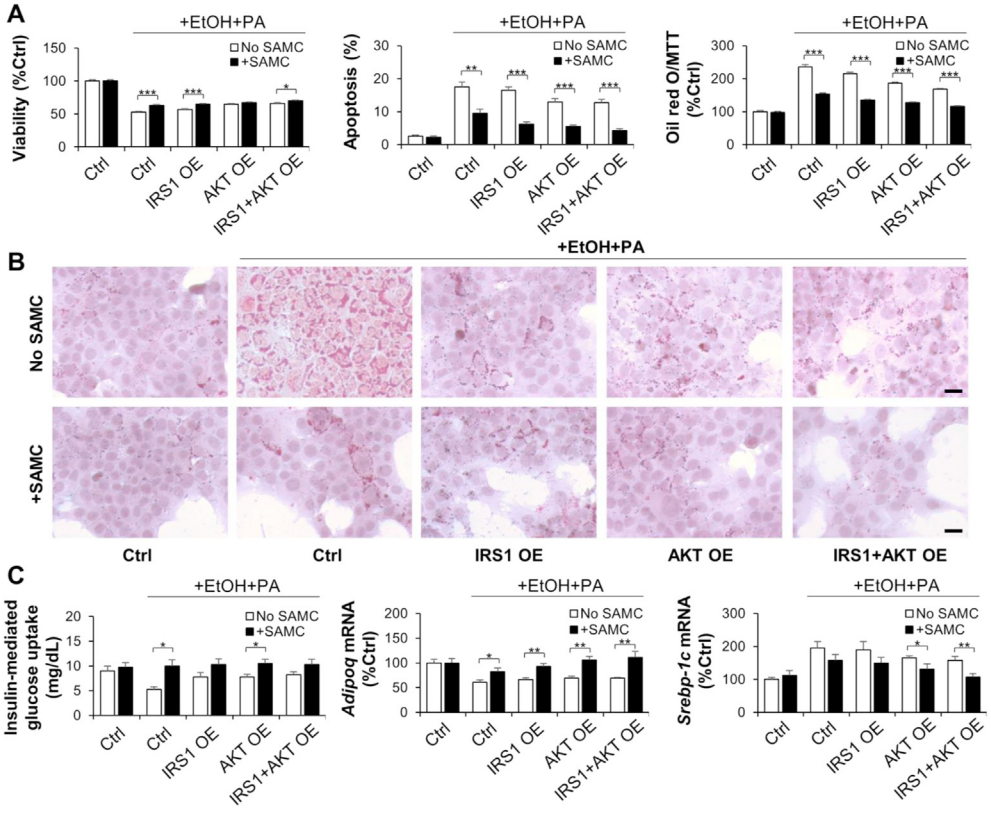

Figure 6 Restoration of the AKT/GSK3β signaling contributed to SAMC-mediated protection *in vitro*. (A) Changes of cell viability, apoptotic ratio, and oil red O staining. (B) Representative oil red O staining images. (C) Changes of glucose uptake ability, *Adipoq*, and *Srebp-1c* mRNAs when AML-12 cells were treated with injury induction combination (palmitate acid + ethanol) and/or SAMC, in the absence or presence of *Irs-1* and/or *Akt* overexpression. Data are expressed as mean ± SEM ($n = 4$). Significant differences between the indicated groups: $^{*}P < 0.05$, $^{**}P < 0.01$, $^{***}P < 0.001$. Scale bar = 50 μm.

although we did not test the concentration of SAMC in the systemic blood flow, a previous study found that SAMC metabolized very quickly and its plasma half-life was less than 5 min in rats (one i.v. injection with 25 mg/kg SAMC, plasma level reduced from ~400 ng/mL at 1 min to ~80 ng/mL at 10 min post injection)[51]. A longer feeding model (*e.g.*, 16-week alcohol feeding, or high fat + alcohol binge) might be better for ALD insulin resistance study. In conclusion, we demonstrated that aged garlic-derived SAMC was an effective treatment agent against chronic ALD-induced cell injury partly *via* direct binding to insulin receptor and restoration of downstream insulin signaling. Potentiation of endogenous insulin signaling, such as the IRS/AKT/GSK3β axis, further contributed to SAMC-mediated hepato-protective effect. To our knowledge, SAMC is the first natural product with direct insulin receptor binding and insulin signaling restoration properties identified by our study. Since long-term administration of SAMC had no detectable adverse effects on healthy mice, we propose that it might be considered an alternative agent for ALD treatment and it could also be explored for future clinical applications and research. Future studies on human cognitive impairments are also warranted.

Acknowledgments

This work was supported by National Natural Science Foundation of China (81970515) and Guangdong Natural Science Funds for Distinguished Young Scholar (2019B151502013, China).

Author contributions

Jia Xiao and George L. Tipoe conceived the study, designed the experiments, and wrote the manuscript. Pingping Luo, Ming Zheng, Rui Zhang, Xiaoming Sun, Wei Li and Qian Yu performed the experiments. Hong Zhang and Yingxia Liu analyzed the data and edited the manuscript. All authors approved the final version of the manuscript.

Conflicts of interest

The authors declare no conflicts of interest.

Appendix A. Supporting information

Supporting data to this article can be found online at https://doi.org/10.1016/j.apsb.2020.11.006.

References

1. Louvet A, Mathurin P. Alcoholic liver disease: Mechanisms of injury and targeted treatment. *Nat Rev Gastroenterol Hepatol* 2015;**12**:231−42.
2. Xiao J, Wang F, Wong NK, He J, Zhang R, Sun R, et al. Global liver disease burdens and research trends: Analysis from a Chinese perspective. *J Hepatol* 2019;**71**:212−21.
3. Liangpunsakul S, Haber P, McCaughan GW. Alcoholic liver disease in Asia, Europe, and North America. *Gastroenterology* 2016;**150**:1786−97.
4. Seitz HK, Bataller R, Cortez-Pinto H, Gao B, Gual A, Lackner C, et al. Alcoholic liver disease. *Nat Rev Dis Primers* 2018;**4**:16.
5. Sofair AN, Barry V, Manos MM, Thomas A, Zaman A, Terrault NA, et al. The epidemiology and clinical characteristics of patients with newly diagnosed alcohol-related liver disease: Results from population-based surveillance. *J Clin Gastroenterol* 2010;**44**:301−7.
6. He J, de la Monte S, Wands JR Wands. Acute ethanol exposure inhibits insulin signaling in the liver. *Hepatology* 2007;**46**:1791−800.
7. de la Monte S, Derdak Z, Wands JR. Alcohol, insulin resistance and the liver−brain axis. *J Gastroenterol Hepatol* 2012;**27 Suppl 2**:33−41.
8. Inoue H. Central insulin-mediated regulation of hepatic glucose production. *Endocr J* 2016;**63**:1−7.
9. Leavens KF, Birnbaum MJ. Insulin signaling to hepatic lipid metabolism in health and disease. *Crit Rev Biochem Mol Biol* 2011;**46**:200−15.
10. He L, Simmen FA, Mehendale HM, Ronis MJ, Badger TM. Chronic ethanol intake impairs insulin signaling in rats by disrupting Akt association with the cell membrane. Role of TRB3 in inhibition of Akt/protein kinase B activation. *J Biol Chem* 2006;**281**:11126−34.
11. Pang M, de la Monte SM, Longato L, Tong M, He J, Chaudhry R, et al. PPARdelta agonist attenuates alcohol-induced hepatic insulin resistance and improves liver injury and repair. *J Hepatol* 2009;**50**:1192−201.
12. Zhu X, Jiang X, Li A, Sun Y, Liu Y, Sun X, et al. *S*-Allylmercaptocysteine suppresses the growth of human gastric cancer xenografts through induction of apoptosis and regulation of MAPK and PI3K/Akt signaling pathways. *Biochem Biophys Res Commun* 2017;**491**:821−6.
13. Li S, Yang G, Zhu X, Cheng L, Sun Y, Zhao Z. Combination of rapamycin and garlic-derived *S*-allylmercaptocysteine induces colon cancer cell apoptosis and suppresses tumor growth in xenograft nude mice through autophagy/p62/Nrf 2 pathway. *Oncol Rep* 2017;**38**:1637−44.
14. Howard EW, Ling MT, Chua CW, Cheung HW, Wang X, Wong YC. Garlic-derived *S*-allylmercaptocysteine is a novel *in vivo* anti-metastatic agent for androgen-independent prostate cancer. *Clin Canc Res* 2007;**13**:1847−56.
15. Wu J, Zhao S, Zhang J, Qu X, Jiang S, Zhong Z, et al. Over-expression of survivin is a factor responsible for differential responses of ovarian cancer cells to *S*-allylmercaptocysteine (SAMC). *Exp Mol Pathol* 2016;**100**:294−302.
16. Liu Y, Yan J, Han X, Hu W. Garlic-derived compound *S*-allylmercaptocysteine (SAMC) is active against anaplastic thyroid cancer cell line 8305C (HPACC). *Technol Health Care* 2015;**23 Suppl 1**:S89−93.
17. Xiao J, Liong EC, Ling MT, Ching YP, Fung ML, Tipoe GL. *S*-Allylmercaptocysteine reduces carbon tetrachloride-induced hepatic oxidative stress and necroinflammation *via* nuclear factor kappa B-dependent pathways in mice. *Eur J Nutr* 2012;**51**:323−33.
18. Xiao J, Ching YP, Liong EC, Nanji AA, Fung ML, Tipoe GL. Garlic-derived *S*-allylmercaptocysteine is a hepato-protective agent in non-alcoholic fatty liver disease *in vivo* animal model. *Eur J Nutr* 2013;**52**:179−91.
19. Xiao J, Guo R, Fung ML, Liong EC, Chang RC, Ching YP, et al. Garlic-derived *S*-allylmercaptocysteine ameliorates nonalcoholic fatty liver disease in a rat model through inhibition of apoptosis and enhancing autophagy. *Evid Based Complement Alternat Med* 2013;**2013**:642920.
20. Xiao J, Xing F, Liu Y, Lv Y, Wang X, Ling MT, et al. Garlic-derived compound *S*-allylmercaptocysteine inhibits hepatocarcinogenesis through targeting LRP6/Wnt pathway. *Acta Pharm Sin B* 2018;**8**:575−86.
21. Bertola A, Mathews S, Ki SH, Wang H, Gao B. Mouse model of chronic and binge ethanol feeding (the NIAAA model). *Nat Protoc* 2013;**8**:627−37.
22. Zeng T, Zhang CL, Zhao N, Guan MJ, Xiao M, Yang R, et al. Impairment of Akt activity by CYP2E1 mediated oxidative stress is involved in chronic ethanol-induced fatty liver. *Redox Biol* 2018;**14**:295−304.
23. Ahn J, Cho I, Kim S, Kwon D, Ha T. Dietary resveratrol alters lipid metabolism-related gene expression of mice on an atherogenic diet. *J Hepatol* 2008;**49**:1019−28.

24. Schümann J, Prockl J, Kiemer AK, Vollmar AM, Bang R, Tiegs G. Silibinin protects mice from T cell-dependent liver injury. *J Hepatol* 2003;**39**:333−40.
25. Brunt EM, Kleiner DE, Wilson LA. Belt P, Neuschwander-Tetri BA; NASH Clinical Research Network (CRN). Nonalcoholic fatty liver disease (NAFLD) activity score and the histopathologic diagnosis in NAFLD: Distinct clinicopathologic meanings. *Hepatology* 2011;**53**: 810−20.
26. Solon-Biet SM, Mitchell SJ, Coogan SC, Cogger VC, Gokarn R, McMahon AC, et al. Dietary protein to carbohydrate ratio and caloric restriction: Comparing metabolic outcomes in mice. *Cell Rep* 2015; **11**:1529−34.
27. Depetris RS, Hu J, Gimpelevich I, Holt LJ, Daly RJ, Hubbard SR. Structural basis for inhibition of the insulin receptor by the adaptor protein Grb14. *Mol Cell* 2005;**20**:325−33.
28. Gondoin A, Hampe C, Eudes R, Fayolle C, Pierre-Eugène C, Miteva M, et al. Identification of insulin-sensitizing molecules acting by disrupting the interaction between the insulin receptor and Grb14. *Sci Rep* 2017;**7**:16901.
29. Wang F, Tipoe GL, Yang C, Nanji AA, Hao X, So KF, et al. *Lycium barbarum* polysaccharide supplementation improves alcoholic liver injury in female mice by inhibiting stearoyl-CoA desaturase 1. *Mol Nutr Food Res* 2018;**62**:e1800144.
30. Singal AK, Kodali S, Vucovich LA, Darley-Usmar V, Schiano TD. Diagnosis and treatment of alcoholic hepatitis: A systematic review. *Alcohol Clin Exp Res* 2016;**40**:1390−402.
31. Bustin SA, Benes V, Garson JA, Hellemans J, Huggett J, Kubista M, et al. The MIQE guidelines: Minimum information for publication of quantitative real-time PCR experiments. *Clin Chem* 2009;**55**:611−22.
32. Zhong W, Zhao Y, Tang Y, Wei X, Shi X, Sun W, et al. Chronic alcohol exposure stimulates adipose tissue lipolysis in mice: Role of reverse triglyceride transport in the pathogenesis of alcoholic steatosis. *Am J Pathol* 2012;**180**:998−1007.
33. Katayama N, Orita M, Yamaguchi T, Hisamichi H, Kuromitsu S, Kurihara H, et al. Identification of a key element for hydrogen-bonding patterns between protein kinases and their inhibitors. *Proteins* 2008;**73**:795−801.
34. Huang CK, Yu T, de la Monte SM, Wands JR, Derdak Z, Kim M. Restoration of Wnt/β-catenin signaling attenuates alcoholic liver disease progression in a rat model. *J Hepatol* 2015;**63**:191−8.
35. Geng Y, Ju Y, Ren F, Qiu Y, Tomita Y, Tomoeda M, et al. Insulin receptor substrate 1/2 (IRS1/2) regulates Wnt/β-catenin signaling through blocking autophagic degradation of dishevelled 2. *J Biol Chem* 2014;**289**:11230−41.
36. Samuel VT, Shulman GI. Mechanisms for insulin resistance: Common threads and missing links. *Cell* 2012;**148**:852−71.
37. Shimomura I, Matsuda M, Hammer RE, Bashmakov Y, Brown MS, Goldstein JL. Decreased IRS-2 and increased SREBP-1c lead to mixed insulin resistance and sensitivity in livers of lipodystrophic and *ob/ob* mice. *Mol Cell* 2000;**6**:77−86.
38. Li Y, Xu S, Mihaylova MM, Zheng B, Hou X, Jiang B, et al. AMPK phosphorylates and inhibits SREBP activity to attenuate hepatic steatosis and atherosclerosis in diet-induced insulin-resistant mice. *Cell Metabol* 2011;**13**:376−88.
39. Samuel VT, Shulman GI. The pathogenesis of insulin resistance: Integrating signaling pathways and substrate flux. *J Clin Invest* 2016; **126**:12−22.
40. Schrieks IC, Heil AL, Hendriks HF, Mukamal KJ, Beulens JW. The effect of alcohol consumption on insulin sensitivity and glycemic status: A systematic review and meta-analysis of intervention studies. *Diabetes Care* 2015;**38**:723−32.
41. Engstler AJ, Aumiller T, Degen C, Dürr M, Weiss E, Maier IB, et al. Insulin resistance alters hepatic ethanol metabolism: Studies in mice and children with non-alcoholic fatty liver disease. *Gut* 2016;**65**: 1564−71.
42. de la Monte SM, Pang M, Chaudhry R, Duan K, Longato L, Carter J, et al. Peroxisome proliferator-activated receptor agonist treatment of alcohol-induced hepatic insulin resistance. *Hepatol Res* 2011;**41**: 386−98.
43. Ozturk ZA, Kadayifci A. Insulin sensitizers for the treatment of non-alcoholic fatty liver disease. *World J Hepatol* 2014;**6**:199−206.
44. Sanyal AJ, Miller V. Regulatory science and drug approval for alcoholic and nonalcoholic steatohepatitis. *Gastroenterology* 2016;**150**: 1723−7.
45. Phillips M, Curtis H, Portmann B, Donaldson N, Bomford A, O'Grady J. Antioxidants *versus* corticosteroids in the treatment of severe alcoholic hepatitis—a randomised clinical trial. *J Hepatol* 2006;**44**:784−90.
46. Moreno C, Langlet P, Hittelet A, Lasser L, Degré D, Evrard S, et al. Enteral nutrition with or without *N*-acetylcysteine in the treatment of severe acute alcoholic hepatitis: A randomized multicenter controlled trial. *J Hepatol* 2010;**53**:1117−22.
47. Luo G, Huang B, Qiu X, Xiao L, Wang N, Gao Q, et al. Resveratrol attenuates excessive ethanol exposure induced insulin resistance in rats *via* improving NAD^+/NADH ratio. *Mol Nutr Food Res* 2017;**61**: 1700087.
48. Testino G, Leone S, Ansaldi F, Borro P. Silymarin and *S*-adenosyl-L-methionine (SAMe): Two promising pharmacological agents in case of chronic alcoholic hepathopathy. A review and a point of view. *Minerva Gastroenterol Dietol* 2013;**59**:341−56.
49. Luo P, Wang F, Wong NK, Lv Y, Li X, Li M, et al. Divergent roles of kupffer cell TLR2/3 signaling in alcoholic liver disease and the protective role of EGCG. *Cell Mol Gastroenterol Hepatol* 2020;**9**: 145−60.
50. Lu Y, Cederbaum AI. CYP2E1 and oxidative liver injury by alcohol. *Free Radic Biol Med* 2008;**44**:723−38.
51. Yang M, Dong Z, Jiang X, Zhao Z, Zhang J, Cao X, et al. Determination of *S*-allylmercaptocysteine in rat plasma by LC−MS/MS and its application to a pharmacokinetics study. *J Chromatogr Sci* 2018;**56**: 396−402.